Development and Characterisation of Completely Degradable Composite Tissue Engineering Scaffolds

PhD Thesis by Montse Charles-Harris Ferrer

PhD Supervisor: Josep A. Planell i Estany

Barcelona, July 2007

Chapter 5. Surface properties of scaffolds produced via Solvent Casting and Phase Separation

Introduction

All materials, and specifically biomaterials, interact with their milieu through their surface. When a biomaterial is implanted into the body, the first molecules to reach the biomaterial surface are the water molecules which get there in nanoseconds. Then, after micro to milliseconds, protein interaction begins; proteins begin to adsorb and resorb on the surface until a protein surface layer is formed. Eventually, cells arrive at the implantation site, attach, spread and begin to proliferate (Figure 5.1). Thus, cells recognise and interact with the protein coating adsorbed onto the biomaterial surface, not with the surface itself. [1;2]. In fact, cells interact by means of specific cell-membrane receptors, often integrins, with defined amino acid sequences in the proteins. The main roles of the integrins, are to attach cells to the extracellular matrix (ECM) and to transduce signals from the ECM to the cells.

The wettability, roughness and surface energy of a biomaterial surface determines its hydrophilic or hydrophobic nature which in turn determines the reactivity of the water layer at the surface of the biomaterial [3]. This water layer directs the composition and conformation of the adsorbed protein layer which will fashion cell attachment, spreading and finally the general host response. If the adsorbed protein layer is non-specific, the host responds by encapsulating the device in a fibrous coating which often compromises the function and long-term success of biomaterials.

A biomaterial must thus possess suitable surface properties which will largely determine its success. Determining the degree of success of a biomaterial is not straightforward due to the variety of mechanical, chemical, biological and even esthetical qualities it must possess. Basically, it can be summarised as being biocompatible or “eliciting a correct host response”, which is the final goal of all biomaterial designs. And the first step towards this host response, before all other properties come into play, is having the appropriate surface properties. Controlling the surfaces of biomaterials is one of the main goals of modern biomaterials science.

Indeed, biological surface science seeks to understand how the properties of a surface control the biological reactivity of cells interacting with that surface in order to tailor surfaces and biomaterials towards greater biocompatibility. The biological environment is however very complex and interactive, making the isolation of meaningful specific phenomena often challenging. Furthermore, the gap between *in vitro* and *in vivo* reactions is ever present. Imitating the richness and complexity of the biological fluids biomaterials will be in contact with in the body is impossible in *in vitro* conditions, thus direct extrapolation and interpretation is not possible. Despite these challenges, understanding the surfaces of biomaterials is a critical part of understanding their biological behaviour.

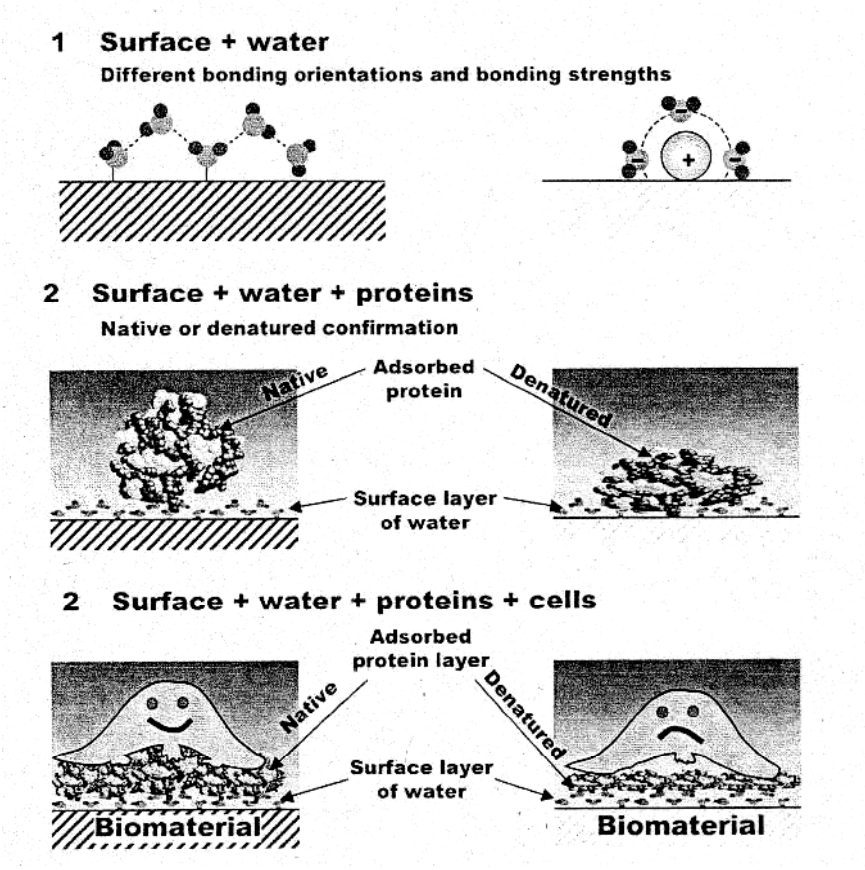

Figure 5.1: Illustration of the sequence of events following the implantation of a biomaterial in the body. First a water shell is formed in nanoseconds. This shell controls the conformation and composition of the layer of adsorbed proteins which in turn determines the cell attachment and spreading behaviour. From [1].

Critical surface properties of biomaterials include charge, wettability, topography, crystallinity and surface energy. The characterisation of these parameters is complex due to the inherent complexity of surface science and to the specific

characteristics and requirements of these materials, such as roughness or the need of humid conditions, but holds the key to obtaining successful biomaterials. [2-5].

Surface wettability is determined by measuring contact angles of various liquids on the surface of a material. Contact angles can be measured by various methods; the most common is the sessile drop method. In the sessile drop method, the contact angle is governed by a balance between the cohesive force of a liquid drop, and the adhesive force of the liquid to the solid surface (Figure 5.3). The information from contact angle measurements is used to compute the hydrophilicity or hydrophobicity of the surface, as well as the surface energy. Negative surface charge has been found to inhibit cell attachment. Hydrophobic surfaces tend to host higher protein adsorption, but the adsorbed proteins seem to be more denatured than on hydrophilic surfaces. Indeed, cell attachment, spreading and cytoskeleton organisation is higher on hydrophilic surfaces. Surface energy has been found to correlate with biocompatibility, although a firm relationship has not been proven. Surface energy is divided into a polar and a dispersive component. The dispersive component is due to the presence of momentary dipoles due to rapid fluctuations of electron densities. The polar component is inherent to the material and is due to the nature of the atomic structure of the material. The polar component can be further divided into an acid and a base component depending on the sign of the charge[2;3;6;7].

Surface topography is the 3D representation of geometric surface irregularities. A surface can be rough or smooth, or curvy or wavy, depending on the magnitude and spacing of the peaks and valleys and how the surface has been produced. In general, roughness refers to the closely spaced irregularities of a surface, whereas waviness refers to the component of texture upon which roughness is superimposed; more widely spaced irregularities (Figure 5. 2).

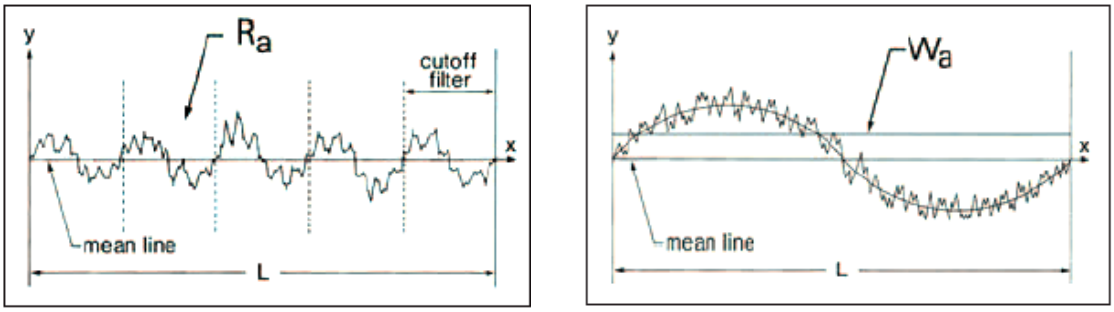

Figure 5. 2: Diagrams illustrating the parameters measured by the interferometer, the roughness, R, corresponds to a one-dimensional reading, (S, corresponds to a two-dimensional reading as used in this study), and W, stands for the waviness of the surface.

Both roughness and waviness make-up surface texture. Surface texture cannot be measured directly and cannot be characterised by a single value. Instead, various parameters must be used in order to illustrate the nature of surface texture. These parameters are classified in three categories. Amplitude parameters are determined solely by deviations from the main profile: peak heights or valley depths, irrespective of their spacing along the surface. They refer to roughness, (R when referring to a profile, S, referring to a surface), or waviness, (W). Spatial parameters are determined only by the spacing of profile deviations along the surface. Hybrid parameters combine both amplitude and spacing in combination[8].

The goal of this study is to characterise the surface properties of the composite scaffolds. The scaffold pore walls are represented by composite films made by skipping the pore-creating step of the scaffold production technique. These composite films are a 2D model of the 3D scaffold structures. The surface morphology, topography, wettability and protein adsorption capacity of the films has been measured. This thorough characterisation is necessary in order to analyse the relationship between surface properties and the biological behaviour of a material (Chapter 6), as well as offering valuable understanding of the material itself.

Materials and Methods

The surface properties of the three-dimensional (3D) composite scaffolds were measured using composite films which represent the pore wall of the three-dimensional scaffolds. These films were made following the same procedure as for the 3D scaffolds skipping the pore-creating step. They present some limitations with respect to the ideal surfaces necessary for most surface characterisations, since they are not smooth, homogeneous nor rigid. They are, however, the closest approximation to the pore wall surface. In order to ensure sound statistical results, a large number of replicas and samples were used for each measurement to compensate for the irregularity of the films.

All measurements were performed with three replicas, and with at least five samples per composition.

The films were characterised using Environmental Scanning Electronic Microscopy (ESEM), their topography was measured by interferometry, their wettability, and surface energy were assessed by contact angle measurement and protein adsorption properties were studied. Various compositions were tested in order to evaluate the surface properties of the solvent-cast and phase-separated scaffolds, and to study the effect of the addition of glass particles and sterilisation.

Composite film preparation

The composite film materials: PLA and G5 glass, have been described in detail in Chapter 2. The solvents used were chloroform (referenced in Chapter 2) for the films representing the solvent cast scaffolds, and dioxane (referenced in Chapter 3) for the films representing the phase-separated scaffolds.

Films made with chloroform: PLA pellets are dissolved in chloroform at a 5 % weight versus volume (w/v) ratio on an orbital shaker. The dissolution takes approximately two days. After complete dissolution, sieved glass particles (< 40μm) were added at 0 weight percent (wt%) , 20 wt% or 50 wt% , the paste was spread onto a Teflon sheet and air-dried for 3 days. Films made with dioxane: 5 % w/v of PLA was dissolved in a mixture of 95% dioxane and 5% water, under magnetic stirring at 50°C overnight. Sieved glass particles were added at 0, 20 and 50 wt% and the paste was then

spread as with the chloroform. In all cases, special care was taken to identify the face of the film which had been exposed to air.

For all measurements, 1cm × 1cm samples were mounted onto glass cover slips using double-faced scotch tape, allowing for easy handling. Ethylene oxide was used to sterilise the samples, both for the surface characterisation and for the protein adsorption assays. The unsterilised samples were cleaned by sonication in distilled water for 10 minutes before each test.

Surface Characterisation

Morphology

The qualitative morphology of the surface was characterised on an Electroscan2020 ESEM, which allows viewing the samples without applying high vacuum or a metallic coating, which could alter surface characteristics. Both the superior and inferior faces of the films were imaged before and after sterilisation. A single sample was viewed per composition.

Topography

The surface topography of the materials was measured with white light interferometry on a WYKO NT1100 interferometer. White light interferometry offers the advantage of being a non-contact system with some lateral resolution, as opposed to perfilometry's very limited lateral resolution. Furthermore, the nature of the films made corrections for tilt, and intrinsic curvature of the surface necessary. These operations are relatively straightforward to perform with the software integrated in the interferometer.

The field of view used for the measurements was 604.4μm × 459.9μm. Three replicas of each composition were tested; five measurements were taken per sample. Both the superior and inferior faces of the films were measured before and after sterilisation.

The recorded parameters were: the roughness average (Sa), the surface kurtosis (Sku), the surface skewness (Ssk,), and the Surface Area Index (SAI). These parameters were chosen in order to have a complete roughness characterisation including amplitude (Sa,Ssk), spatial (Sku) and hybrid (SAI) roughness parameters (Table 5.1).

Parameter name	Formula	Definition
Residual surface	$\eta(x,y)$	**Residual surface**: the surface remaining after filtering to remove the tilt, or curvature of the sample
Sa	$S_a = \frac{1}{MN}\sum_{j=1}^{N}\sum_{i=1}^{M}\lvert\eta(x_i, y_j)$, where M and N = nº of data points in x and y	The r**oughness average** is useful for detecting variations in overall surface height
Sq	$S_q = \sqrt{\frac{1}{MN}\sum_{j=1}^{N}\sum_{i=1}^{M}\eta^2(x_i, y_j)}$	The **root mean square roughness** represents the standard deviation of the profile
Ssk	$S_{sk} = \frac{1}{MNS_q^3}\sum_{j=1}^{N}\sum_{i=1}^{M}\eta^3(x_i, y_j)$	**Skewness**, measures the asymmetry of the profile about the mean plane. Ssk<0 : predominance of valleys Ssk>0 : predominance of peaks
Sku	$S_{ku} = \frac{1}{MNS_q^4}\sum_{j=1}^{N}\sum_{i=1}^{M}\eta^4(x_i, y_j)$	**Kurtosis** measures the spikiness of the surface, or randomness of surface heights Sku>3: spiky surface Sku<3: bumpy surface Sku=3 : perfectly random surface

Table 5.1: Definitions and formulas of the roughness parameters used to characterise the surfaces in this study

Sa, represents, the mean spacing between adjacent local peaks or the arithmetic mean of the absolute value of the surface departures from the mean plane. It is a relatively stable parameter in the sense that a single non-typical peak or valley will be averaged out and have only a small influence on the final value. It does not detect any differences in the spacing of the features though, and thus markedly different surfaces can have the same Sa value. Sku, provides information on the "spikiness" or peakedness of a surface. Sku values are high when a high proportion of the surface falls within a narrow range of heights. It is also a measure of the randomness of surface height. A perfectly Gaussian or random surface will have a Sku of 3, the more repetitive the surface features are, the farther the value is from 3. Sku is very sensitive to outliers in the surface data. Ssk measures the asymmetry of the surface about the mean plane. The predominance of bumps or peaks will have a positive Ssk, whereas the predominance of holes or valleys will have a negative Ssk. As was the case with the Sku, Ssk is very sensitive to outliers on the surface. Finally, SAI is the ratio between the surface area of the sample and the area of the field of view. It is a very stable parameter.

Contact Angle and Surface Energy

The wettability and surface energy of the samples were measured using the sessile drop technique on a Dataphysics Contact Angle System OCA15Plus. The sessile drop technique allows the characterisation of the solid-liquid contact angle under static conditions, and is simple to perform. 3μl droplets of the measuring liquid were used in an atmospherically controlled chamber at room temperature.

Three replicas of each composition were tested, with three to eight droplets per sample. The angle was measured five seconds after coming in contact with the material. Measurements for all compositions were performed randomly.

The contact angles were measured with ultrapure distilled water, GYBCO's Dulbecco Modified Eagle medium (DMEM) with 10% Fetal Calf Serum (FCS), and diodomethane. A polar and an apolar liquid are needed in order to compute the surface energy of the materials by means of their wettability results. Water and diodomethane are a polar and an apolar liquid respectively. The DMEM + 10% FCS is a polar liquid; it contains water, proteins, sugars and other organic components. It was used in order to assess the influence of these organic components on the contact angle of the surface. Furthermore, it is the medium the materials will be immersed in during cell culture.

The results for the contact angles measured with water (polar) and diodomethane (apolar) were used to calculate the surface energy of the films using the following equation:

$$\gamma_{sv} = \gamma_{sl} + \gamma_{lv} \cos\theta \qquad \{1\}$$

Where γ_{sv} stands for the energy of the surface, γ_{sl}, stands for the interfacial tension between the solid and the drop, γ_{lv}, stands for the liquid-vapour surface tension[9;10], and $cos\theta$ is the contact angle of the drop with the surface as shown in Figure 5.3.

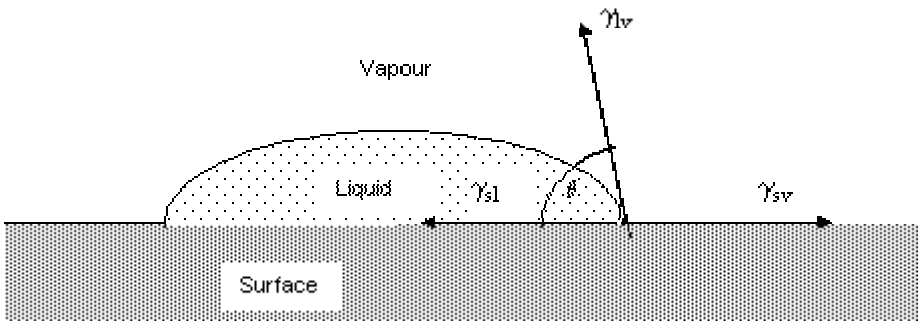

Figure 5.3: Schema of the sessile drop contact angle system.

Protein adsorption

A preliminary protein adsorption assay was performed by measuring the amount of protein adsorbed after one-hour incubation in DMEM with 10% FCS. 6mm diameter discs were cut out of each sample and immersed in 400 μl of DMEM+10%FCS for 1 hour at 37°C. After incubation, samples were rinsed in phosphate buffered saline (PBS) in order to remove loosely adsorbed proteins, and transferred to clean test tubes. The adsorbed proteins were desorbed by adding 200 μl of 5% sodium dodecyl sulphate into each tube, the tubes were left overnight at 37°C under orbital shaking. The amount of adsorbed protein was measured with a Bicinchoninic acid (BCA) Protein Assay Reagent Kit (PIERCE). The absorbance data was referenced to a bovine albumin serum standard.

Five samples of each composition were tested.

Statistics

The statistical significance of the differences between the averages of the results for all parameters studied was calculated using ANOVA tables with a Fisher multiple comparison test. Statistical significance was established at $p < 0.05$. These calculations have been performed with MINTAB^{TM} Release 14 Minitab Inc. software.

Results whose difference is not statistically significant are indicated with a horizontal line on the graphs. When values are not alongside eachother, they are indicated with a symbol (*, +).

Results

Morphology

ESEM images of the upper face of the films showed a homogeneous distribution of the glass particles throughout their surface (Figure 5.4 and Figure 5.5). The glass particles on the surface of the chloroform films are exposed due to the polymer film peeling off the glass particle, this can be seen clearly in Figure 5.4c and e. For dioxane-dissolved films, the polymer seems to coat the glass particles more evenly (Figure 5.5c, e). The inferior faces, in contact with the Teflon sheet, were imprinted with the imperfections of the Teflon sheet they had been dried on and seem, qualitatively, less rough than the superior faces (see Figure App5.1 and 5.2 in the Appendix Chapter 5).

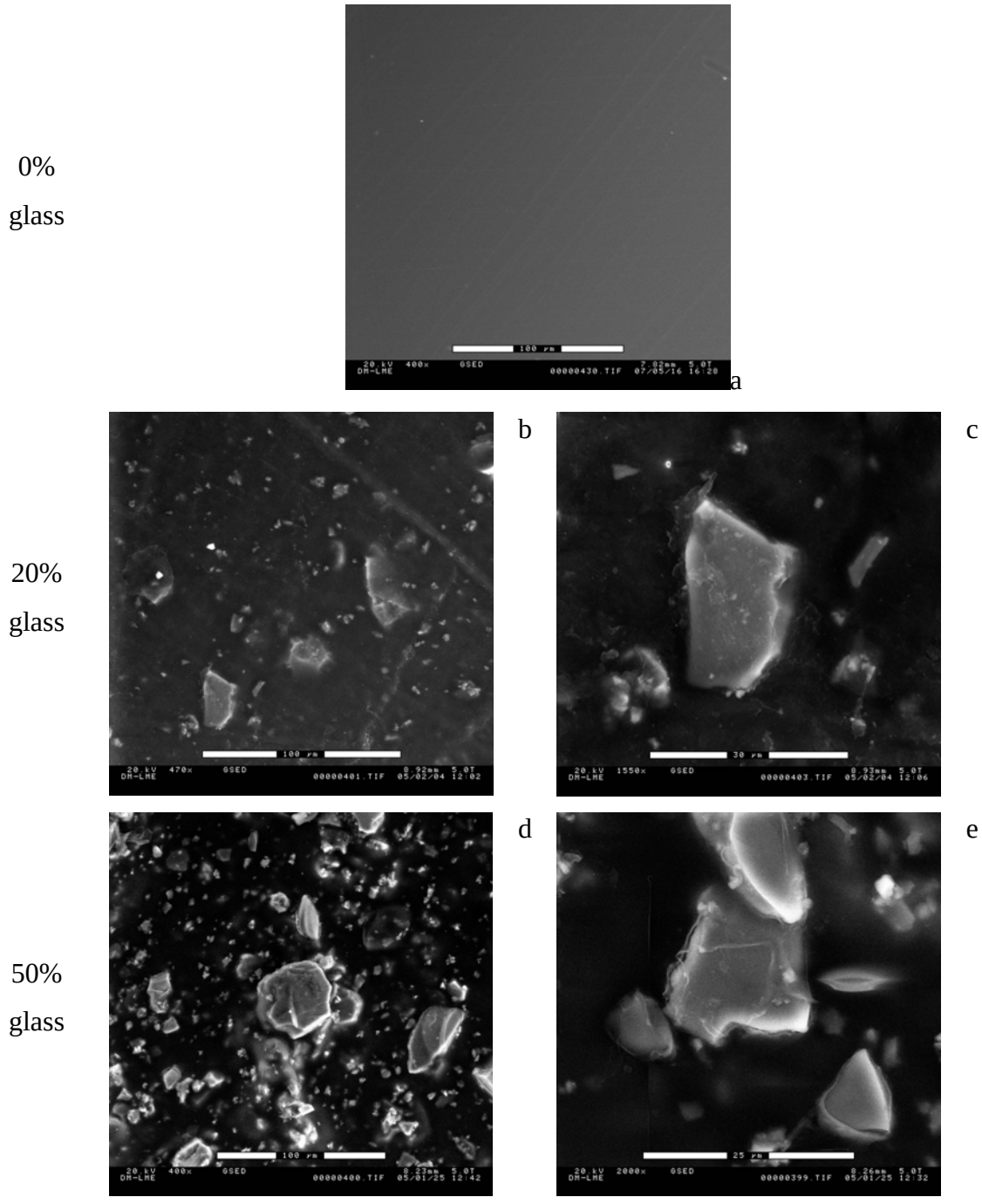

Figure 5.4 : ESEM images of the upper surface of the composite films made of PLA dissolved in chloroform with 0%, 20% and 50 wt% glass particles. Close-up images (c and e) show the polymer peeling off the glass particles. (Scale bars a), b) and d) correspond to 100μm, scale bars c) and e) correspond to 30μm and 25μm respectively)

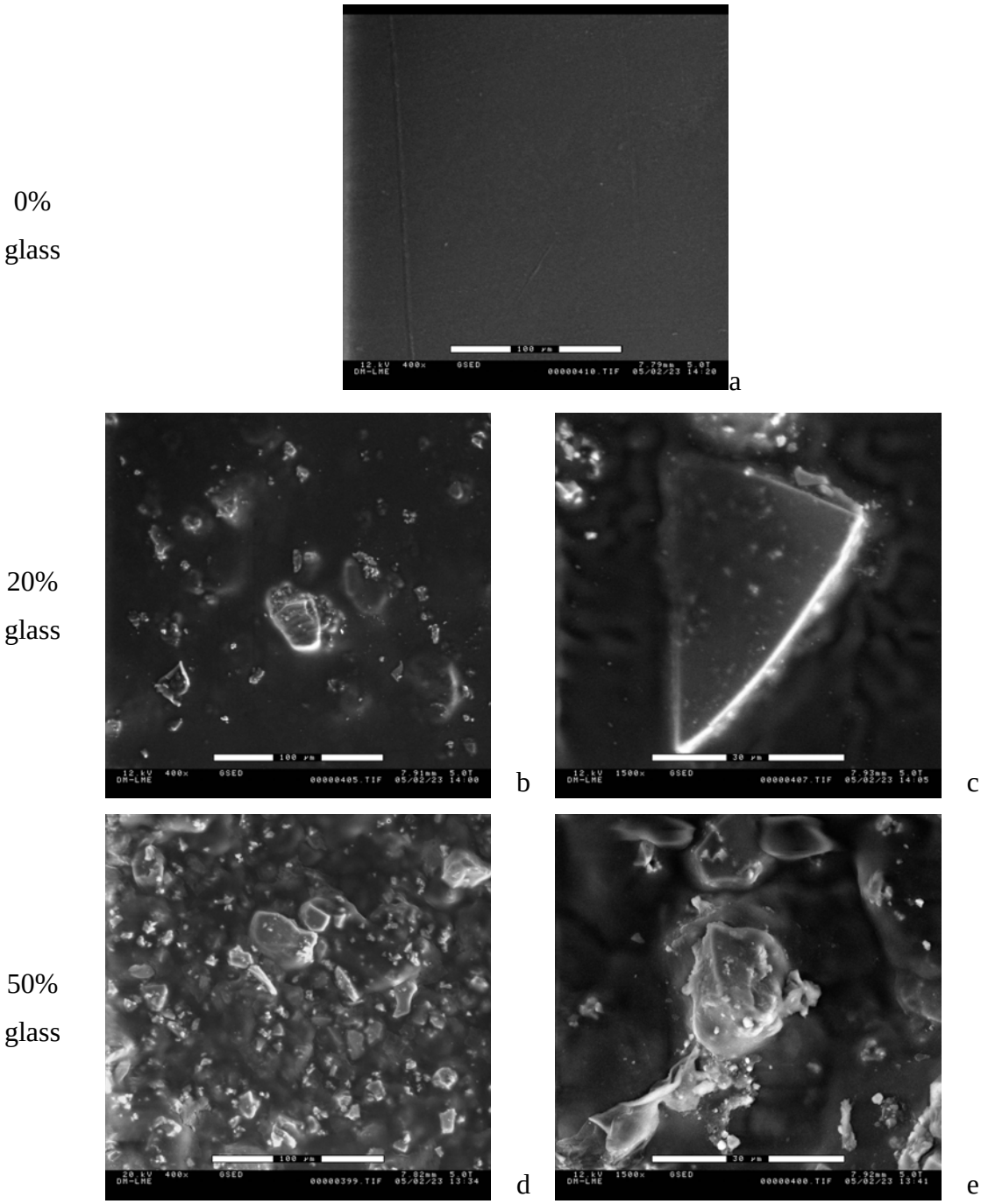

Figure 5.5: ESEM images of the upper surface of the composite films made of PLA dissolved in dioxane with 0%, 20% and 50 wt% glass particles. The polymer seems to coat the superficial glass particles without peeling in the close-up images (c and e). (Scale bars a), b) and d) correspond to 100μm, scale bars c) and e) correspond to 30μm)

Roughness

Various roughness parameters of the films were measured using white light interferometry. This technique also allows for a qualitative morphological evaluation of the surface as can be seen in Figure 5.6. These images are in good agreement with the ESEM images above, thus the interferometric readings were accurate and were not distorted by artificial features.

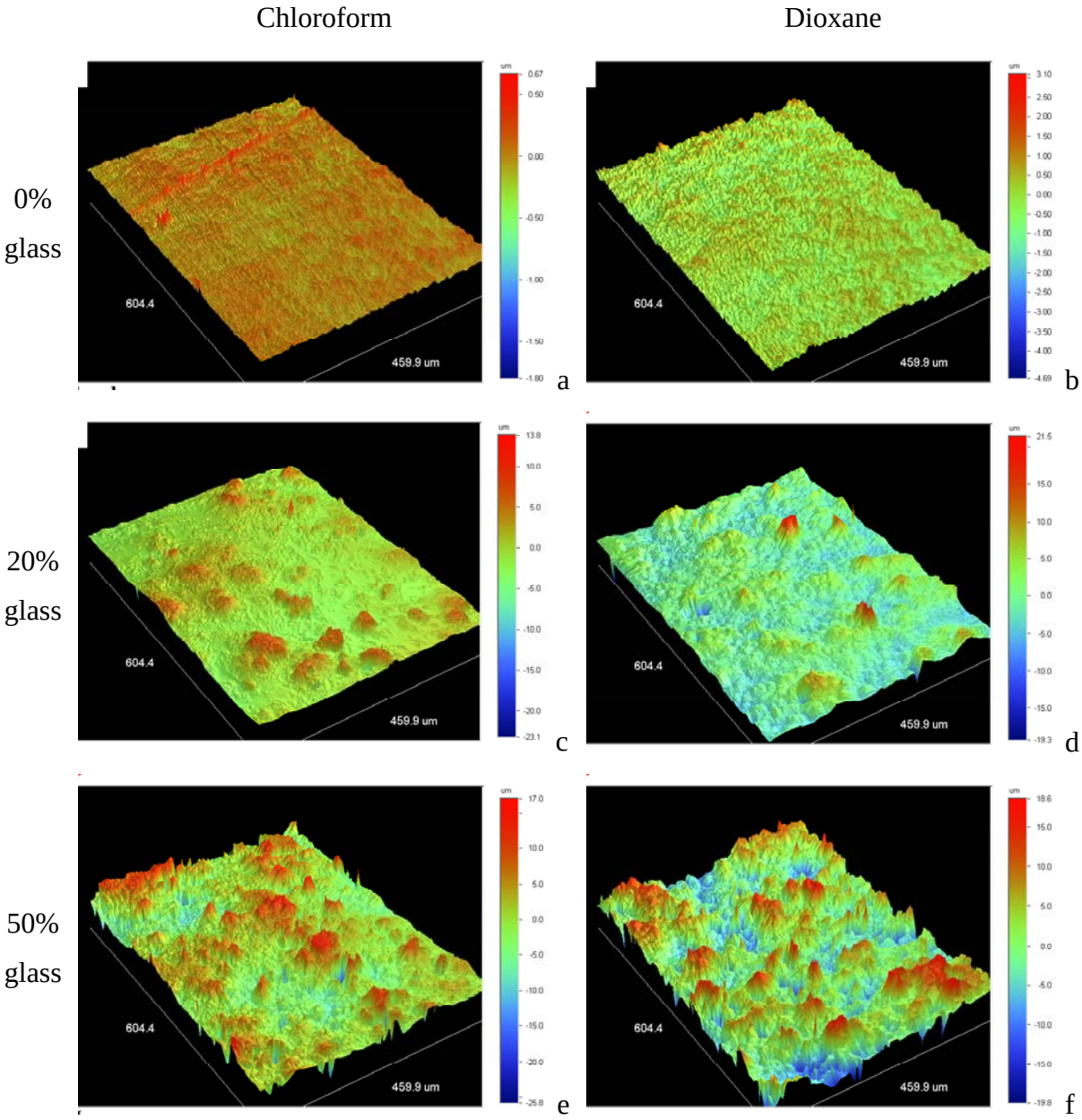

Figure 5.6: Interferometry images of the upper surface of the composite films dissolved in chloroform (C) and dioxane (D) with different glass weight percents, a) 0%C, b) 0%D, c) 20%C, d) 20%D, e) 50%C, f) 50%D **.** (Note: scale bars are not identical).

Quantitatively, the effect of the glass particles is clear on the Sa and SAI parameters (Table 5.2, Figure 5.7 and Figure 5.8): it increases the roughness of the films. The films made using dioxane as a solvent had a higher Sa than those made with chloroform. The superior and inferior faces of the films had different roughnesses (see Table App5.1 in Appendix Chapter 5). For films with 20% or 50% glass, the face in contact with the Teflon sheet gave lower roughness values, whereas for films without glass, the inferior face was slightly rougher (Figure 5.9) probably due to the imperfections of the Teflon sheet that produce roughness. It is interesting to note that the Sa measured for the inferior faces of the 0%C and 0%D sheets gave very similar results. This would of course be expected given that both readings represent the roughness due to the Teflon sheets. This result adds weight to the interferometry measurements, and indicates they are representative despite their variability. Sterilisation did not have a significant effect on the surface roughness of the films (see Table App5.2 in the Appendix Chapter 5).

The Ssk and Sku parameters are difficult to interpret due to the large standard deviations they present. This variability is due to the sensitivity of the parameters to outliers or extreme features on the surface topography. As was explained in the Materials and Methods section, a singular feature on the measured surface can change the value of Ssk and Sku entirely. These features can be due to a speck of dust or a scratch made during manipulation. The calculation of statistical significance loses meaning with such large standard deviations. It is interesting to note, however, that the Ssk and Sku values for the sterilised films follow the same trend as for the unsterilised films, thus adding some weight to their significance (see Table App5.2 in the Appendix Chapter 5).

Taking these limitations into account, Sku and Ssk do give additional information on the surface characteristics. Sku decreases as the wt% of glass increases, thus composite films are less “peaked” than PLA-only films. Or in other words, the distribution of peaks on the 50wt% glass films is more Gaussian or random than on pure PLA films. This is logical since the 0% films, should not have peaks at all, thus, those measured are surely due to extraordinary elements. Indeed, the standard deviations of the Sku of the 0% films, are disproportionate. The distribution of the glass particles on the 50wt% films is therefore more random than on the 20wt% films.

The Ssk results show that all surfaces except 0% films are relatively symmetric. Indeed values for the 20wt% and 50wt% glass particle films, are all almost null and have small standard deviations. 50 wt% films have negative Ssk values, thus valleys and pits predominate, whereas 20wt% films have positive Ssk values, thus peaks predominate. 0wt% films again have very high standard deviations, and thus the values are surely due to outliers on the surfaces.

Composition	Sa (nm)	Sku	Ssk	SAI
0%C	74.41 ± 32	189.16 ± 366	-3.36 ± 8	1.01 ± 0.01 *
20%C	1491.81 ± 218	12.36 ± 5	0.156 ± 0.6	1.09 ± 0.02
50%C	3806.71 ± 587	5.01 ± 1	-0.407 ± 0.5	1.53 ± 0.16
0%D	253.10 ±71	36.33 ± 55	0.28 ± 3	1.02 ± 0.03 *
20%D	1963.22 ± 319	8.91 ± 3	0.418 ± 0.6	1.13 ± 0.03
50%D	4659.56 ± 388	3.57 ± 0.5	-0.067 ± 0.3	1.63 ± 0.11

Table 5.2: Roughness parameters of the upper faces of the composite films. Sa= spacing between local peaks, Sku = kurtosis of the surface, Ssk = skewdness of the surface plane, and SAI = surface area index. *: the differences between the SAI of 0%C and 0%D are not statisticallly significant.

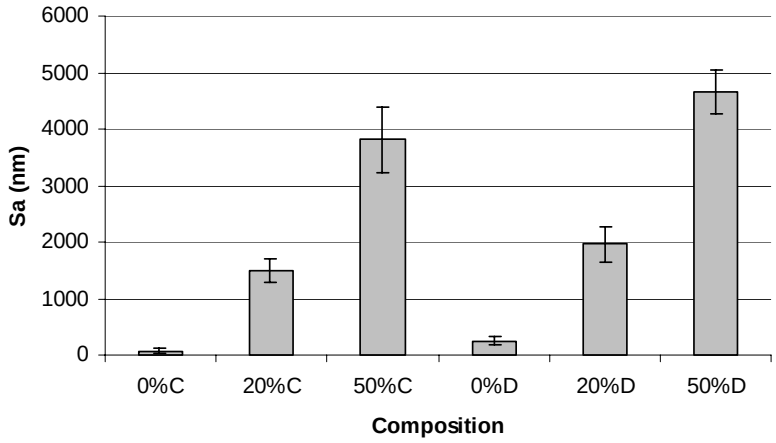

Figure 5.7: Surface roughness, Sa, of the composite films. The compositions include films made using chloroform (C) as a solvent, or dioxane (D), and with 0%, 20% or 50% glass weight percent.

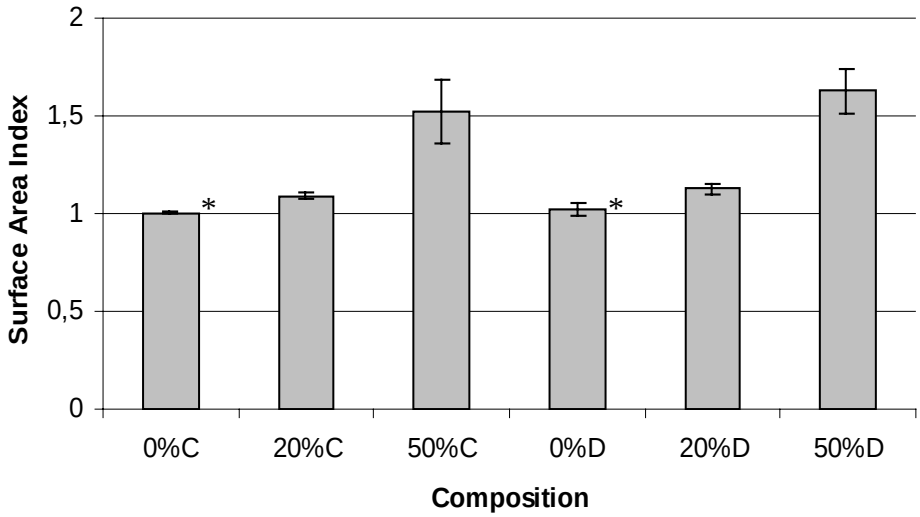

Figure 5.8: Surface Area Index of the composite films. The compositions include films made using chloroform (C) as a solvent, or dioxane (D), and with 0%, 20% or 50% glass weight percent.
*: the differences between the SAI of 0%C and 0%D are not statisticallly significant.

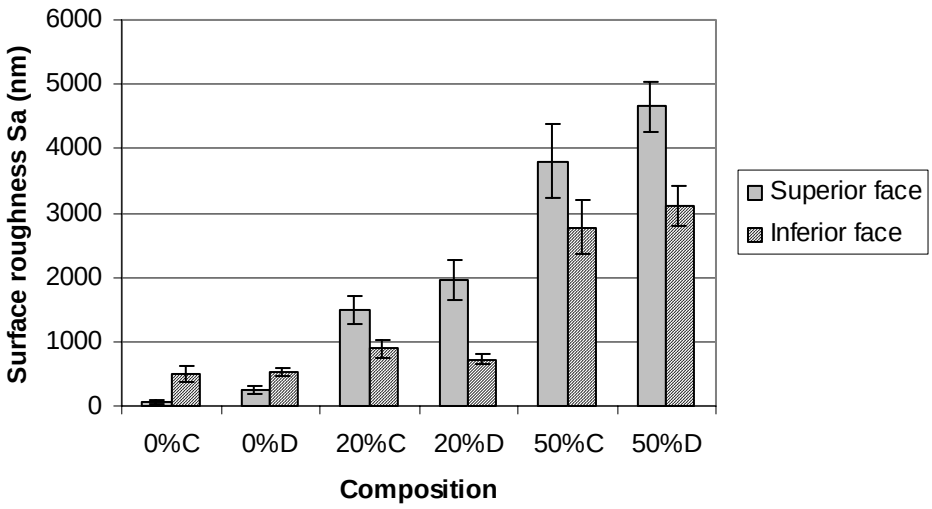

Figure 5.9: Comparison between the roughness (Sa) of the superior and inferior (in contact with Teflon sheet) faces of the composite films. The compositions include films made using chloroform (C) as a solvent, or dioxane (D), and with 0%, 20% or 50% glass weight percent.

Contact Angle and Surface Energy

The contact angle results for the films showed different trends for films made using chloroform as a solvent and those dissolved in dioxane. The measurements made using either water or DMEM + 10% FCS, which are both polar liquids, followed similar trends.

Results using water or DMEM +10%FCS as contact liquids. For films made with chloroform, the glass particles increased the hydrophilicity of the films (decreased the contact angle), whereas for dioxane films the contrary occurred, i.e. contact angles increased with increasing glass wt% (Figure 5.10 and Figure 5.11). This trend was statistically significant for all compositions except for the differences between 0%C and 20%C, and 0%D and 20%D measured with water.

The contact angles measured with DMEM+10%FCS were lower than those measured with water. Sterilisation decreased the contact angle of the films when measured with either water or DMEM + 10%FCS . This decrease was statistically significant in all cases except for compositions 20%D and 50%D measured with DMEM +10%FCS.

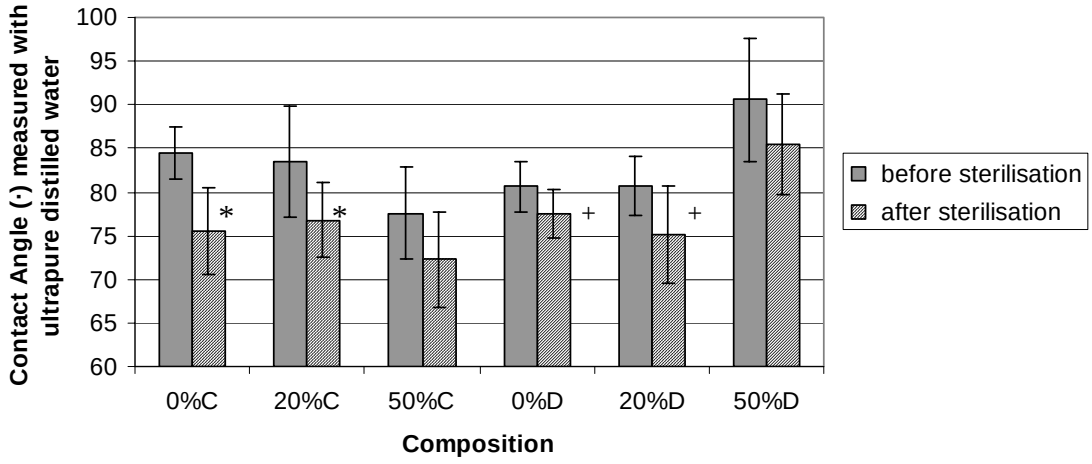

Figure 5.10: Contact angle values measured with ultrapure distilled water on composite films before and after sterilisation with ethylene oxide. The compositions include films made using chloroform (C) as a solvent, or dioxane (D), and with 0%, 20% or 50% glass weight percent.

*,+: the differences between readings for 0%C and 20%C, and 0% and 20%D are not statistically significant.

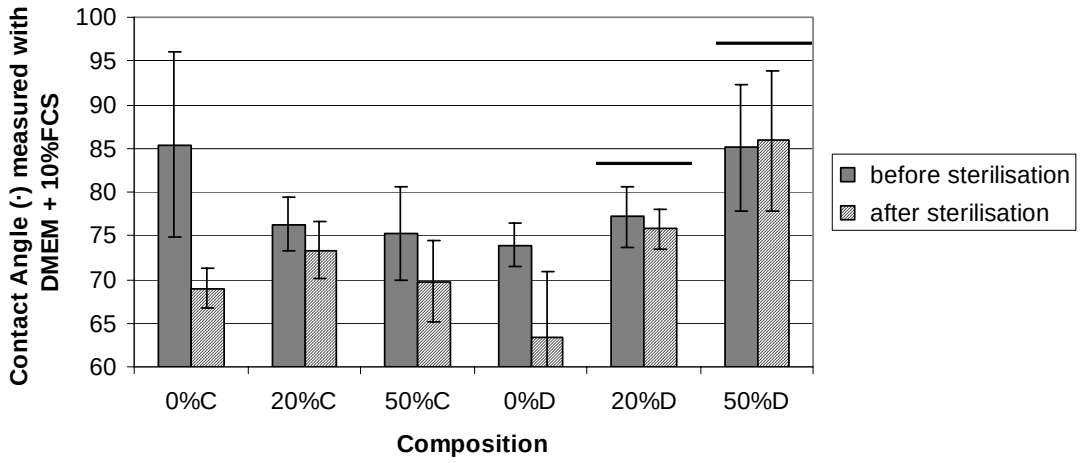

Figure 5.11: Contact angle values measured with DMEM + 10% FCS on composite films before and after sterilisation with ethylene oxide. The compositions include films made using chloroform (C) as a solvent, or dioxane (D), and with 0%, 20% or 50% glass weight percent.

The contact angle results can be analysed as a three-factor experiment design. Using for example, the contact angle measurements with ultrapure distilled water, the influence of three factors : a) glass wt%, b) solvent type and c) sterilisation can be analysed.

	Glass wt%	Solvent Type	Sterilisation
Low level (-1)	0%	chloroform	Yes
High level (+1)	50%	dioxane	No

Table 5.3: Levels of the factors used for the 2^3 experiment design analysis of the contact angle with ultrapure distilled water.

The experiment design analysis reveals that the interaction between solvent type and glass wt%, the effect of the solvent type and the effect of the sterilisation were all significant factors. For the sake of clarity, the detailed calculations of the factorial experiment design can be seen in the Appendix Chapter 5. The linear model would read as follows:

Contact Angle = 80.51 + 3.52×Glass wt%×Solvent + 3.042× Solvent -2.80×Sterilis. {2}

where Glass wt% stands for the weight percent of glass particles in the scaffolds, Solvent stands for the solvent type, either chloroform or dioxane, and Sterilis. for the either sterilised or unsterilised. The values for Glass wt%, solvent type and sterilisation correspond to the levels shown in Table 5.3.

The effect of the interaction coincides with the previous qualitative and quantitative interpretations: for films dissolved in chloroform (X2=-1), increasing the glass wt% (X1) decreases the contact angle, for films dissolved in dioxane (X2=+1) on the other hand, increasing the glass wt% increases the contact angle (Figure 5.12). Furthermore, dioxane-dissolved films had higher contact angles than chloroform-dissolved ones (Figure 5.13), and sterilisation tends to decrease the contact angle of all films (Figure 5.14).

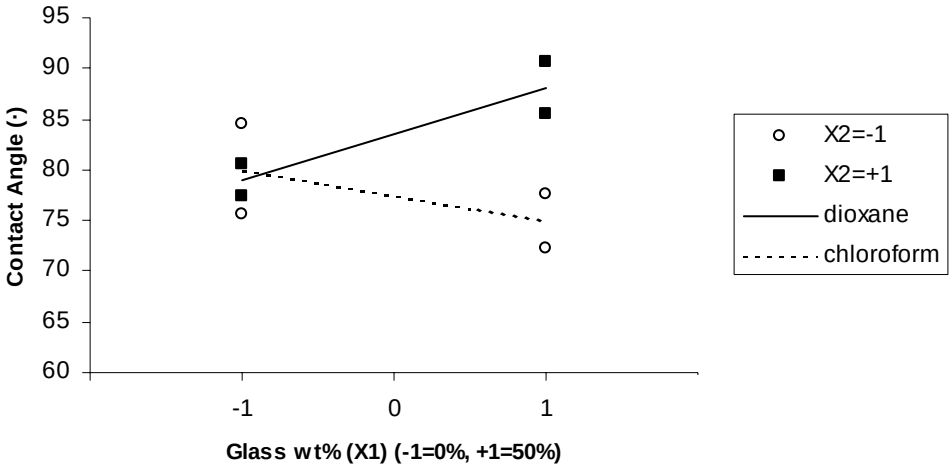

Figure 5.12: Effect of the interaction between the Glass wt% (X1) and the Solvent Type (X2) on the contact angle of the composite films measured with ultrapure distilled water.

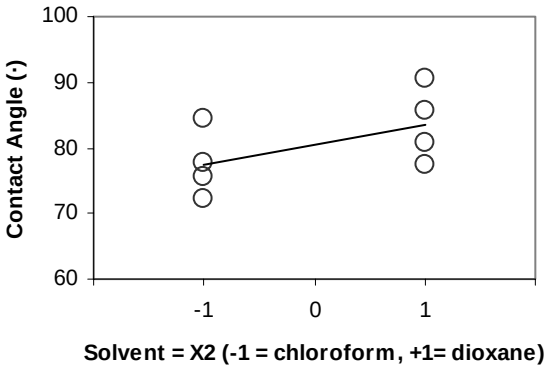

Figure 5.13: Effect of the solvent type (X2) on the contact angle of the composite films measured with ultrapure distilled water.

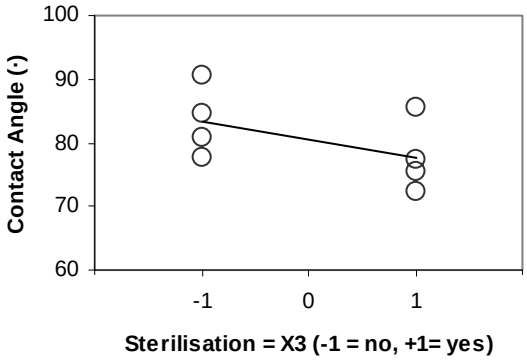

Figure 5.14: Effect of the sterilisation (X3) on the contact angle of the composite films measured with ultrapure distilled water.

Results using diodomethane. The contact angle of the chloroform films decreased with glass wt%, although there were no significant differences between compositions 20%C and 50%C. For dioxane films, the highest contact angle was measured on 20%D (Figure 5.15). Interestingly, sterilisation tended to increase the contact angle measured with diodomethane, although the difference was only significant for the films dissolved in dioxane.

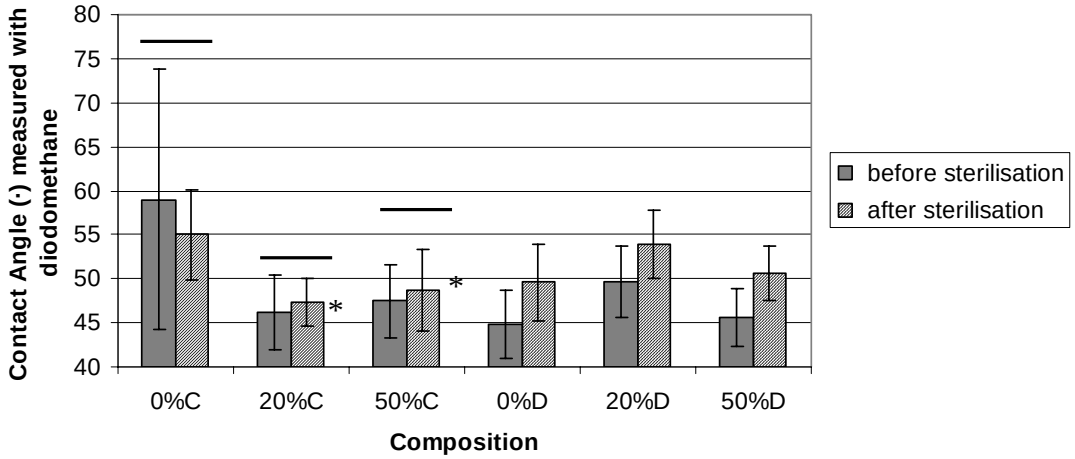

Figure 5.15: Contact angle values measured with diodomethane on composite films before and after sterilisation with ethylene oxide. The compositions include films made using chloroform (C) as a solvent, or dioxane (D), and with 0%, 20% or 50% glass weight percent. *: the differences between readings for 20%C and 50%C are not statistically significant.

Surface energy. Figure 5.16 shows the surface energy of the composite films after sterilisation. For the films dissolved using chloroform as a solvent, a higher glass content tends to increase the surface energy. For films dissolved using dioxane, the composition with 50 wt% glass tends to have a lower surface energy than the composition without glass or with 20 wt% of glass. The differences are not statistically significant however. Sterilisation tended to increase the surface energy of the materials dissolved in chloroform, but its effect on the dioxane-dissolved materials is not clear.

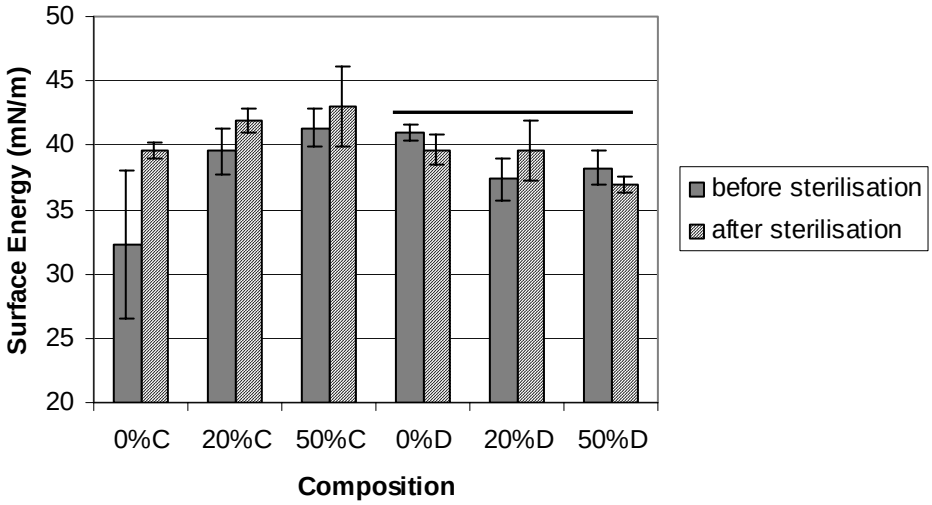

Figure 5.16: Surface energy of the composite films before and after sterilisation. The compositions include films made using chloroform (C) as a solvent or dioxane (D), and with 0%, 20% or 50% glass weight percent. The differences between 0%D, 20%D and 50%D are not statistically significant.

If the surface energy is decomposed into its dispersive and polar components, the effect of sterilisation can be further analysed. In effect, sterilisation with ethylene oxide increases the polar component of the surface energy of all the composite materials substantially (Figure 5.17) and tends to decrease the dispersive component of the surface energy significantly in the case of films made with dioxane.

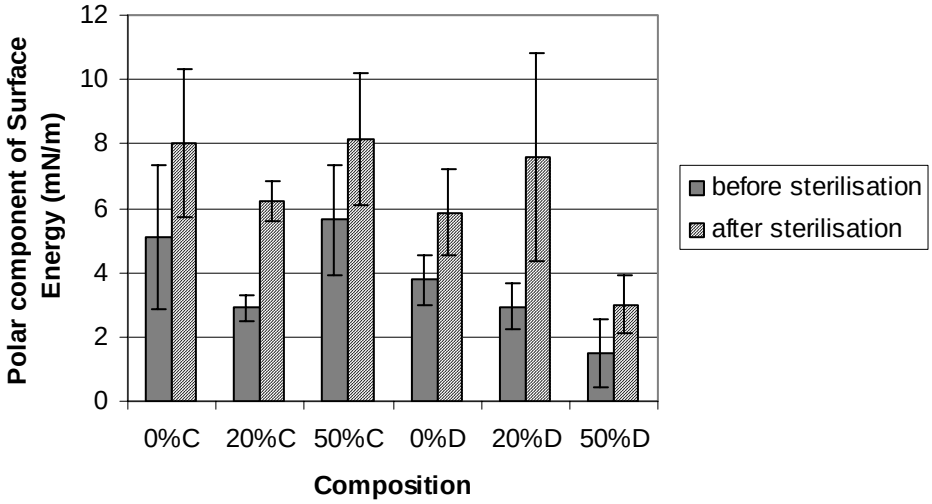

Figure 5.17: Polar component of the surface energy of the composite films before and after sterilisation with ethylene oxide. The compositions include films made using chloroform (C) as a solvent or dioxane (D), and with 0%, 20% or 50% glass weight percent.

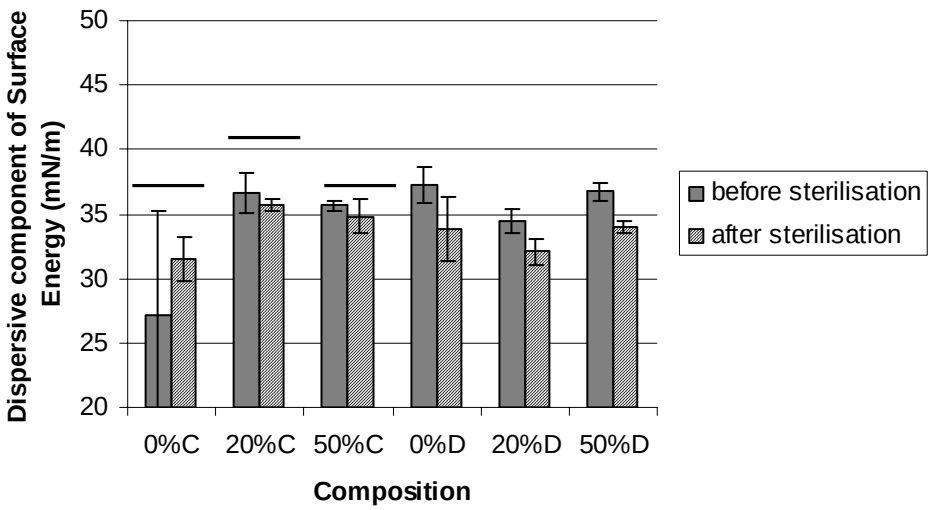

Figure 5.18: Dispersive component of the surface energy of the composite films before and after sterilisation with ethylene oxide. The compositions include films made using chloroform (C) as a solvent or dioxane (D), and with 0%, 20% or 50% glass weight percent.

Protein adsorption

The total amount of protein adsorbed onto the 6mm discs, in μg/ml, is shown in Figure 5.19. For all materials, the total amount of adsorbed protein increases significantly with glass wt%. If the total protein is normalised with the surface area index (SAI) of the superior and inferior surfaces of the films, the amount of protein in μg/cm^2 is obtained (Figure 5.20). For the chloroform films, composition 50%C has a larger protein concentration. For the dioxane films, however, the differences between the compositions are no longer statistically significant, though they follow the same trend.

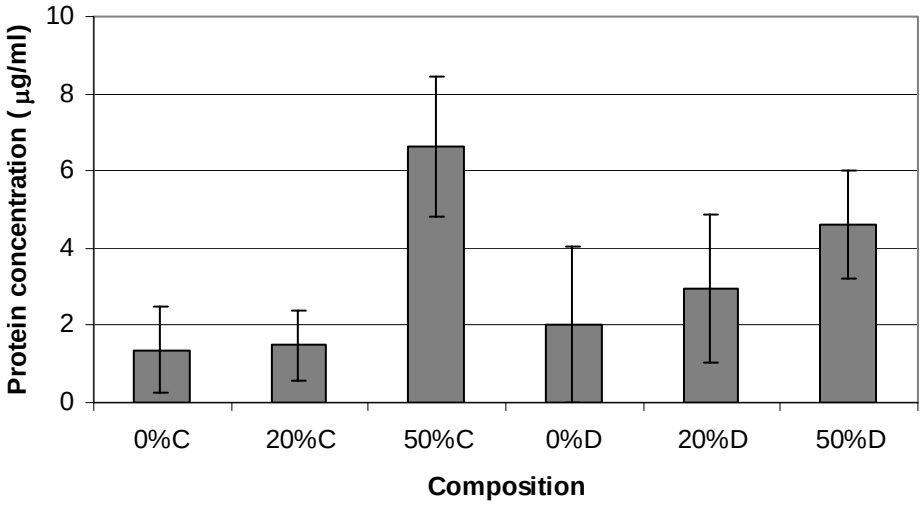

Figure 5.19: Total protein adsorption (μg/ml) of the composite materials. The compositions include films made using chloroform (C) as a solvent or dioxane (D), and with 0%, 20% or 50% glass weight percent.

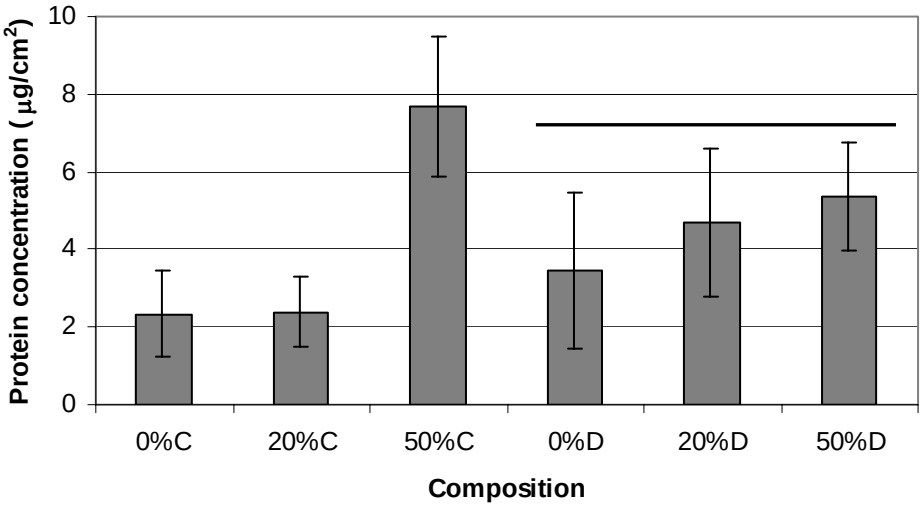

Figure 5.20: Total protein adsorption (µg/cm^2) normalised with the surface area index (SAI) of the composite materials. The compositions include films made using chloroform (C) as a solvent or dioxane (D), and with 0%, 20% or 50% glass weight percent. The differences between 0%D, 20%D and 50%D are not statistically significant.

Discussion

The field of surface characterisation is inherently complex. This complexity stems from sample requirements, the characterisation measurement itself, and the registered parameters. Contact angle measurements can be used as an example to illustrate this fact: a) contact angles should ideally be measured on smooth, rigid, chemically and physically inert surfaces which are often difficult to achieve without altering the surface meaningfully, b) the accuracy of the results depends on the quality of the surface, the skill of the experimenter, the purity of the measuring liquid and its interaction with the surface, and c) the contact angle can be measured statically or dynamically, and its value changes with time [11;12].

The same can be applied to roughness measurements, which require a large range of parameters for adequate characterisation [5;13-15]. The results listed on Table 5.2 exemplify this fact. For a given composition, certain parameters such Sa and Sku, which are very sensitive to outliers in the surface data, have large scatterings, whereas SAI, a hybrid parameter, is very stable.

Comparing materials which vary in composition further increases this complexity. A change in composition, for example, can affect both the chemistry and the morphology of a surface, and it may also influence the surface energy, heterogeneity or stiffness. Thus, it is important to establish a well-defined protocol in order to obtain reproducible results, and even so, one should expect high dispersion.

In addition to the challenges of surface characterisation, this study is also subject to the irregularity of the films used, and the limitation of their extrapolation to the 3D structure. Indeed, the films are meant to represent the pore walls of the scaffold, although their processing, thickness and manipulation are somewhat different. The composite films are, however, the closest approximation to the pore-wall material of the 3D scaffold. Lück et al. [16] and Jee et al. [17] use a similar approach to characterise the surface of microspheres and tissue engineering constructs respectively. The results must thus be interpreted more as a tool to understand scaffold properties and behaviour which can then be used to characterise scaffold properties.

The results indicate that the solvent used to make the films determines the coating of the glass particles on the surface of the films (Figure 5.4 and Figure 5.5). Although this observation is qualitative, it explains the different trends in wettability, surface energy and protein adsorption observed between chloroform and dioxane-dissolved films. The degree of coating of the glass particles is probably due to the hydrophilic properties of the materials involved, their wettability in other words. In effect, the soluble calcium phosphate glass used in this study is highly hydrophilic (Contact Angle with H_2O = 28.9°), and water is infinitely soluble in dioxane, but only slightly soluble in chloroform (0.02 w/w). Thus, the PLA dissolved in the water and dioxane mixture coats the superficial glass particles better than when it is dissolved in chloroform.

Thus, in the case of the chloroform-dissolved films, most of the superficial glass particles are exposed and therefore influence both the chemistry and the roughness of the surface. The contact angle measurements for these films reflect the hydrophilic effect of the glass particles on the surface (Figure 5.10, Figure 5.12). In the case of the dioxane films, however, most of the glass particles are coated with polymer, which means they contribute mainly to the roughness of the surface, increasing the material's hydrophobicity. This result can be related to Rupp et al.'s [18] conclusions on the relationship between roughness and hydrophobicity which state that roughness increases the hydrophobicity of hydrophobic materials. The interpretation of these conclusions depends, however, on the definition of hydrophobicity. For Rupp et al., in reference to titanium, the limit between hydrophobicity and hydrophilicity lies at 90°, whereas Vogler [3] defines a hydrophobic material was one with a water contact angle $\theta > 65°$, in reference to biomaterials in general. The fact that dioxane tends to increase the contact angle of the films (Figure 5.13) can also be related to the effect of roughness on hydrophobicity. As can be seen in Figure 5.9, dioxane-dissolved films have higher roughness and higher contact angles than chloroform-dissolved films.

Sterilisation has an important effect on the surface characteristics of the materials (Figure 5.10, Figure 5.14). The composite films become more hydrophilic by treatment with ethylene oxide. Interestingly, surface energy calculations indicate that sterilisation mainly affects the polar component of the surface energy (Figure 5.17). The correlation between surface energy and biological interaction, including protein

adsorption, is often stated in the literature [3;11], and its polar component is thought to play a role in cell behaviour [19]. Furthermore, cell adhesion has been found to depend on different sterilisation treatments [20;21]. Other sterilisation methods, such as gamma radiation or autoclave would affect the surface properties of the materials differently, and must be taken into account when changing the sterilisation protocol.

The preliminary protein adsorption assay results confirms the trends observed in previous experiments. The protein adsorption pattern on the materials can be related to the coating of the glass particles on their surface as well. Before normalisation with SAI (if the concentration is measured in μg/ml) an increase in glass wt% increases the protein adsorption for all film compositions (Figure 5.19). After normalisation with SAI, there are no longer statistical differences between the dioxane film compositions, (on which most of the glass particles are coated with polymer) (Figure 5.20). For chloroform films, however, the exposed glass particles influence protein adsorption significantly.

Protein adsorption seems to be sensitive to the effect of the exposed glass particles, but less sensitive to the effect of the roughness (or at least to this magnitude of roughness), than other surface characterisation parameters studied. In fact, it correlates well to the surface energy results (Figure 5.16). Protein adsorption is related to the surface composition, wettability, charge and roughness [17;22;23]. In competitive protein environments, such as in this study, the concentration and nature of the protein layer on the material is known to change with time in what is known as the Vroman effect [24]. Cell behaviour depends not only on the nature of the adsorbed protein layer, but also on the surface characteristics below the layer, which in turn affect the conformation and viability of the adsorbed proteins [6;25;26].

The results of the surface characterisation generate a large amount of data which could be analysed and compared in various ways. It would be interesting, for example, to analyse the effect of sterilisation on the polymer and on the glass particles, or how the various roughness parameters reflect the coating of the glass particles. Caution must be exercised when analysing the data however, due to the large scattering of the results. As mentioned previously, the limitations of this study include the complexity and large

degree of scatter inherent to surface characterisations and the film-model as an imitation of the pore wall material.

Conclusions

- A thorough characterisation of the surface properties of composite films has been performed in this study.
- The solvent type, glass weight content and sterilisation influence the wettability, surface energy and protein adsorption capacity of the materials.
- The addition of the soluble calcium phosphate glass changes both the morphology and the physico-chemistry of the surface of the material and affects protein adsorption. The effect of the glass particles depends on their degree of coating by the PLA.
- The coating of the glass particles is greater for dioxane-dissolved films than for chloroform-dissolved films. Coating by PLA reduces the chemical effects of the glass particles. Thus, the presence of glass particles increase the hydrophilicity of the films when they are made with chloroform, but the contrary is true when they are made with dioxane.
- Films made with dioxane exhibit higher surface roughness than those made with chloroform.
- Surface energy and protein adsorption results correlate.
- In Chapter 2, the optimum composition was chosen so that the glass particles were not too tightly bound within the polymer matrix, and could thus influence the chemical and biological properties of the scaffolds. This was achieved using a mixture of dioxane and water as a solvent. The results of this study (Chapter 5) further confirm this solvent choice.
- The results include a degree of scattering inherent to the characterisation of rough and irregular surfaces. Despite this fact, this information can be used to interpret and understand the biological behaviour of the three-dimensional scaffolds made of this composite material.

- The complete characterisation of the surface properties of these composite materials will be a valuable tool to couple with cell culture assays in order to understand their biological behaviour (Chapter 6).

Publications

The results of this study have been published in:

"Surface characterisation of completely degradable composite scaffolds"
M.Charles-Harris, M.Navarro, E.Engel, M.P.Ginebra, J.A.Planell
Journal of Materials Science: Materials in Medicine 2005; vol 16, pp 1125-30

Bibliography

(1) Kasemo B. Biological Surface Science. Surface Science 2002; 500:656-677.

(2) Castner DG, Ratner BD. Biomedical surface science: Foundations to frontiers. Surface Science 2002; 500:28-60.

(3) Vogler EA. Structure and reactivity of water at biomaterial surfaces. Advances in Colloid and Interface Science 1998; 74:69-117.

(4) Tirrell M, Kokkoli E, Biesalski M. The role of surface science in bioengineered materials. Surface Science 2002; 500:61-83.

(5) von Recum AF, Brown CE, Shannon CE, LaBerge M. Surface Topography. Handbook of biomaterials evaluation. Scientific, Techincal and Clinical Testing of Implant Materials. 2005.

(6) Webb K, Hlady V, Tresco PA. Relative importance of surface wettability and charged functional groups on NIH 3T3 fibroblast attachment, spreading, and cytoskeletal organization. J Biomed Mater Res 1998; 41(3):422-430.

(7) Morra M, Cassinelli C. Bacterial adhesion to polymer surfaces: a critical review of surface thermodynamic approaches. J Biomater Sci Polym Ed 1997; 9(1):55-74.

(8) Schaffer GH. The Many Faces of Surface Texture. American Machinist and Automated Manufacturing 1988; 55:61-68.

(9) Mulqueen M, Huibers PDT. Measuring Equilibrium Surface Tensions. In: Krister Holmberg, editor. Handbook of Applied Surface and Colloid Chemistry Volume 2. Wiley and Sons., 2001: 217-224.

(10) Lam CNC, Lu JJ, Neumann AW. Measuring Contact Angle. In: Krister Holmberg, editor. Handbook of Applied Surface and Colloid Chemistry Vol. 2. Wiley and Sons. Ltd., 2001: 251-279.

(11) Ratner BD. Surface Properties and Surface Characterization of Materials. In: Ratner BD, Hoffman AS, Schoen FJ, Lemons JE, editors. Biomaterials Science. Elsevier Academic Press, 2004: 40-59.

(12) Lam C.N., Lu J., Neumann W. Measuring contact angle. In: Krister Homberg, editor. Handbook of applied surface and colloid chemistry. Chalmers university of technology, Göteborg, Sweden.: John Wiley and sons,ltd, 2001: 251-280.

(13) Stout KJ, Blunt L, . Surface Topography. 2nd ed. London: Penton Press, 2000.

(14) Dong WP, Sullivan PJ, Stout KJ. Comprehensive study of parameters for characterizing three-dimensional surface topography I: Some inherent properties of parameter variation. Wear 1992; 159:161-171.

(15) Stout KJ, Blunt L. Nanometres to micrometres: three-dimensional surface measurement in bio-engineering. Surface and Coatings Technology 1995; 71:69-81.

(16) Luck M, Pistel KF, Li YX, Blunk T, Muller RH, Kissel T. Plasma protein adsorption on biodegradable microspheres consisting of poly(D,L-lactide-co-glycolide), poly(L-lactide) or ABA triblock copolymers containing poly(oxyethylene). Influence of production method and polymer composition. J Control Release 1998; 55(2-3):107-120.

(17) Jee KS, Park HD, Park KD, Kim YH, Shin JW. Heparin conjugated polylactide as a blood compatible material. Biomacromolecules 2004; 5(5):1877-1881.

(18) Rupp F, Scheideler L, Rehbein D, Axmann D, Gels-Gerstorfer J. Roughness induced dynamic changes of wettability of acid etched titanium implant modifications. Biomaterials 2004; 25(7-8):1429-1438.

(19) Ponsonnet L, Reybier K, Jaffrezic N, Comte V, Lagneau C, Lissac M, Martelet C. Relationship between surface properties (roughness, wettability) of titanium and titanium alloys and cell behaviour. Materials Science & Engineering C-Biomimetic and Supramolecular Systems 2003; 23(4):551-560.

(20) Anselme K. Osteoblast adhesion on biomaterials. Biomaterials 2000; 21(7):667-681.

(21) Charles-Harris M, Navarro M, Engel E, Aparicio C, Ginebra MP, Planell JA. Surface characterization of completely degradable composite scaffolds. J Mater Sci Mater Med 2005; 16(12):1125-1130.

(22) Ying PQ, Yu Y, Jin G, Tao ZL. Competitive protein adsorption studied with atomic force microscopy and imaging ellipsometry. Colloids and Surfaces B-Biointerfaces 2003; 32(1):1-10.

(23) McFarland CD, Thomas CH, DeFilippis C, Steele JG, Healy KE. Protein adsorption and cell attachment to patterned surfaces. J Biomed Mater Res 2000; 49(2):200-210.

(24) McFarland CD, Mayer S, Scotchford C, Dalton BA, Steele JG, Downes S. Attachment of cultured human bone cells to novel polymers. J Biomed Mater Res 1999; 44(1):1-11.

(25) Lee JW, Kim YH, Park KD, Jee KS, Shin JW, Hahn SB. Importance of integrin beta1-mediated cell adhesion on biodegradable polymers under serum depletion in mesenchymal stem cells and chondrocytes. Biomaterials 2004; 25(10):1901-1909.

(26) Lenza RF, Jones JR, Vasconcelos WL, Hench LL. In vitro release kinetics of proteins from bioactive foams. J Biomed Mater Res 2003; 67A(1):121-129.